

1 Supplementary material

The $\Lambda_b^0 K^-$ mass spectra are shown with a wider bin width. Also shown are the $\Xi_b(6227)^0$ and $\Xi_b(6227)^-$ mass spectra with the same mass window of 304 MeV, also presented as absolute mass. For these plots, the mass and widths of the peaks are fixed to the values obtained from the nominal fits in the paper. Lastly, we show a comparison of recent Ξ_b^- mass measurements.

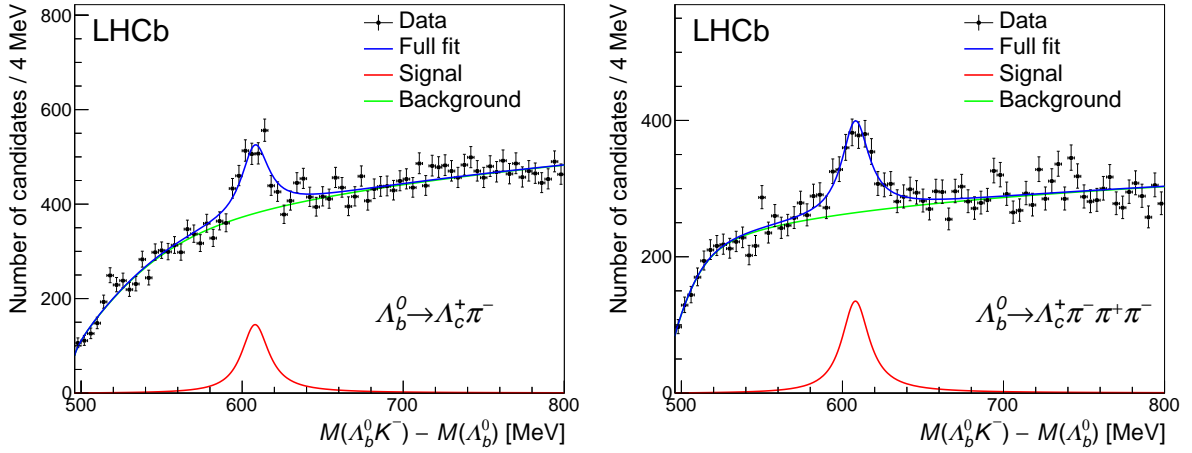


Figure 1: Distribution of $\delta M_K = M(\Lambda_b^0 K^-) - M(\Lambda_b^0)$ for (left) $\Lambda_b^0 \rightarrow \Lambda_c^+ \pi^-$ and (right) $\Lambda_b^0 \rightarrow \Lambda_c^+ \pi^- \pi^+ \pi^-$ signal candidates in 4 MeV wide bins. The fit is overlaid.

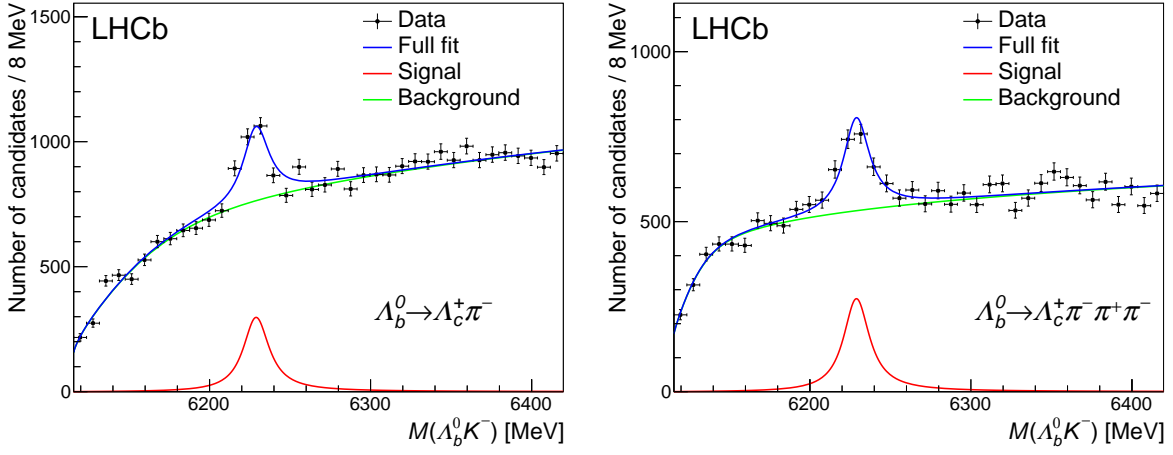


Figure 2: Distribution of $M(\Lambda_b^0 K^-)$ for (left) $\Lambda_b^0 \rightarrow \Lambda_c^+ \pi^-$ and (right) $\Lambda_b^0 \rightarrow \Lambda_c^+ \pi^- \pi^+ \pi^-$ signal candidates in 8 MeV wide bins. The fit is overlaid.

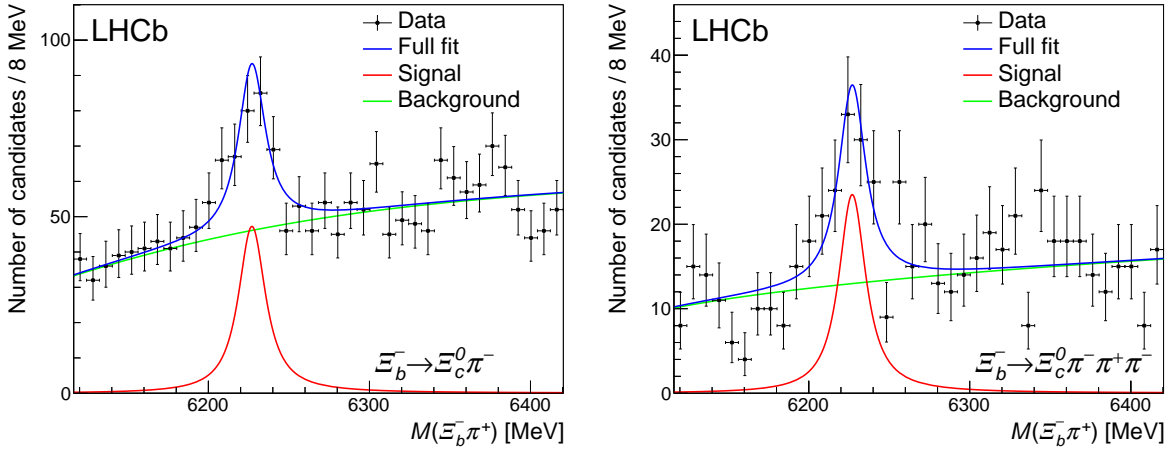


Figure 3: Distributions of $M(\Xi_b^- \pi^+)$ with (left) $\Xi_b^- \rightarrow \Xi_c^0 \pi^-$ and (right) $\Xi_b^- \rightarrow \Xi_c^0 \pi^- \pi^+ \pi^-$ decays in 8 MeV wide bins. The fit is overlaid.

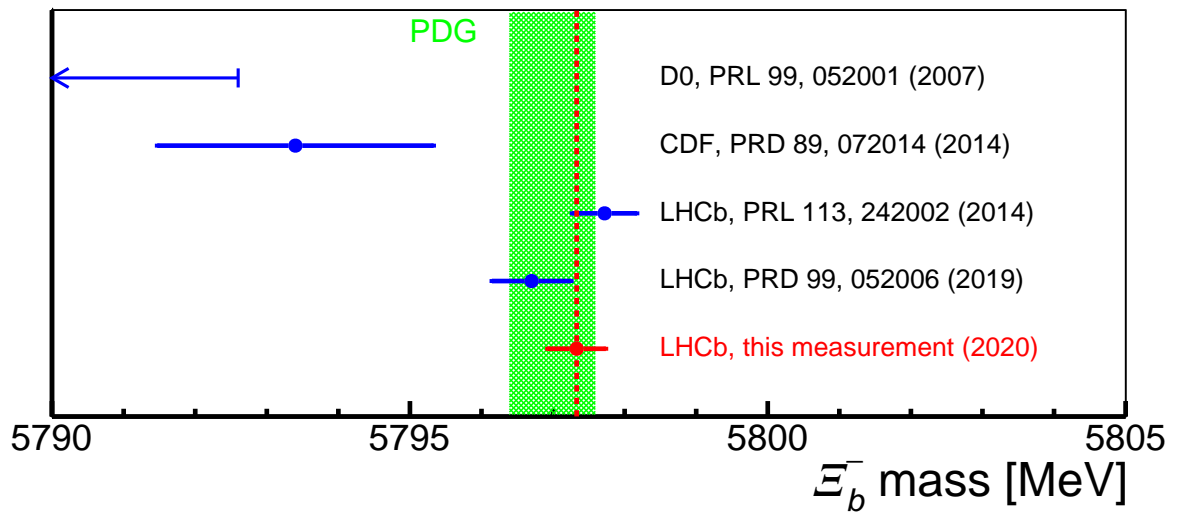


Figure 4: Comparison of the recent (blue) Ξ_b^- mass measurements used in the PDG average (green), along with the measurement presented in this paper (red). The green band shows the current PDG average.